Study of the Thermal Diffusion Behavior of Alkane/Benzene Mixtures by Thermal Diffusion Forced Rayleigh Scattering Experiments and Lattice Model Calculations

Pavel Polyakov,[†] **Jutta Luettmer-Strathmann,**[‡] **and Simone Wiegand*,**[†]

Forschungszentrum Jülich GmbH, IFF−Weiche Materie, D-52428 Jülich, Germany, and Department of Physics and Department of Chemistry, The University of Akron, Akron, Ohio 44325-4001

In this work the thermal diffusion behavior of binary mixtures of linear alkanes (heptane, nonane, undecane, tridecane, pentadecane, heptadecane) in benzene has been investigated by thermal diffusion forced Rayleigh scattering (TDFRS) for a range of concentrations and temperatures. The Soret coefficient S_T of the alkane was found to be negative for these *n*-alkane/benzene mixtures indicating that the alkanes are enriched in the warmer regions of the liquid mixtures. For the compositions investigated in this work, the magnitude of the Soret coefficient decreases with increasing chain length and increasing alkane content of the mixtures. The temperature dependence of the Soret coefficient depends on mixture composition and alkane chain length; the slope of S_T versus temperature changes from positive to negative with increasing chain length at intermediate compositions. To study the influence of molecular architecture on the Soret effect, mixtures of branched alkanes (2-methylhexane, 3-methylhexane, 2,3-dimethylpentane, 2,4-dimethylpentane, 2,2,3-trimethylbutane, and 2,2,4-trimethylpentane) in benzene were also investigated. Our results for the Soret coefficients show that the tendency for the alkanes to move to the warmer regions of the fluid decreases with increasing degree of branching. The branching effect is so strong that for 2,2,4-trimethylpentane/benzene mixtures the Soret coefficient changes sign at high alkane content and that equimolar 2,2,3-trimethylbutane/benzene mixtures have positive Soret coefficients in the investigated temperature range. In order to investigate the effect of molecular interactions on thermal diffusion, we adapted a recently developed two-chamber lattice model to *n*-alkane/benzene mixtures. The model includes the effects of chain-length, compressibility, and orientation dependence of benzene−benzene interactions and yields good qualitative predictions for the Soret effect in *n*-alkane/benzene mixtures. For the branched isomers, we find some correlations between the moments of inertia of the molecules and the Soret coefficients. PACS numbers: 66.10.Cb, 61.25.Hq

I. Introduction

Thermal diffusion or the so-called Ludwig−Soret effect describes the coupling between a temperature gradient and a resulting mass flux. The effect has important technical applications for example in the modeling of the separation of crude oil components under the influence of thermal diffusion in geological conditions;[1−3] it also plays an important role in separation techniques for liquid mixtures (see, e.g., refs 4−6).

According to the phenomenological equations of irreversible thermodynamics, thermodiffusion in a binary fluid mixture is described by the flux of one of the components in response to a temperature and concentration gradient.[7] For an alkane/benzene mixture, for example, the flux ***J*** of the alkane in response to a temperature gradient ∇T and a mass-fraction gradient ∇w may be written as[7]

$$\boldsymbol{J} = -\rho D\nabla w - \rho D_T w(1 - w)\nabla T \qquad (1)$$

where w is the mass fraction of the alkane, ρ is the density of the mixture, D is the mutual diffusion coefficient, and D_T is the thermal diffusion coefficient of the alkane. In the steady state ($J = 0$) the concentration gradient is characterized by the

Soret coefficient $S_T = D_T/D$ of the alkane; a positive Soret coefficient of the alkane corresponds to the alkane moving to the colder regions of the fluid.[8,9]

Thermal diffusion in liquid mixtures of nonpolar fluids is known to reflect a range of microscopic properties such as the mass, size, and shape of the molecules as well as their interactions (see ref 6 for a review). In mixtures of polar liquids, specific interactions between the molecules dominate the thermal diffusion process while mass and size of the molecules are most important in Lennard-Jones fluids. For liquids of nonpolar molecules that are more complex than Lennard-Jones fluids, the Soret effect appears to depend on a delicate balance of the molecular properties of the components.

This is true, in particular, for mixtures of alkanes and aromatic solvents. Debuschewitz and Köhler[10] investigated thermal diffusion in isotopic mixtures of benzene and cyclohexane and found that the Soret coefficient could be written as a sum of three contributions:

$$S_T = a_M \delta M + b_I \delta I + S_T^0 \qquad (2)$$

where $\delta M = (M_1 - M_2)(M_1 + M_2)^{-1}$ and $\delta I = (I_1 - I_2)(I_1 + I_2)^{-1}$ are the relative differences of the masses (M_1, M_2) and moments of inertia (I_1, I_2) of the molecules, respectively. The coefficients a_M and b_I were found to be independent of the composition of the mixture. The third contribution, S_T^0, reflects

* Corresponding author phone: 49-2642 616654; fax: 49-2641 612280; e-mail: s.wiegand@fz-juelich.de.
† Forschungszentrum Jülich GmbH.
‡ The University of Akron.

chemical differences of the molecules and was found to depend on the concentration and change its sign at a benzene mole fraction of 0.7. A further investigation of the isotope effect[11] suggested that the absolute rather than the relative differences between the masses and moments of inertia should enter the expression for the Soret coefficient so that the difference terms in eq 2 are given by $\delta M = M_1 - M_2$ and $\delta I = I_1 - I_2$.

A number of studies have focused on the Soret effect in mixtures containing an alkane or benzene as one of the components. Different experimental techniques were applied to investigate the thermal diffusion behavior of toluene/hexane,[12−14] alkane/alkane,[15,16] cyclohexane/benzene,[10] and *n*-alkane/benzene[13,17−21] mixtures. Recently, alkane/alkane and methyl-naphthalene/alkane mixtures have been investigated systematically.[22] The three binary mixtures of dodecane, isobutylbenzene and 1,2,3,4 tetrahydronaphthalene[23] were the subject of a benchmark study to provide reliable values for the Soret, diffusion, and thermal diffusion coefficients of these mixtures. Rowley et al.[24,25] measured the heat of transport of binary mixtures of six alkanes (*n*-hexane, *n*-heptane, *n*-octane, 3-methylpentane, 2,3-dimethylpentane, 2,2,4- trimethylpentane) with chloroform and tetrachloride in a wide concentration range at 30 °C. Demirel and Sandler[26] combined these data to determine values of thermal diffusion ratios, $K_T = w(1 - w)S_T$, for these mixtures. They found that branching had a very small effect on the thermal diffusion ratios. For mixtures of pentane and decane, Perronace et al.[15] determined Soret coefficients from both experiment and molecular dynamics simulations and found reasonable agreement between experiment and simulations.

Thermal diffusion in hydrocarbon mixtures has also been investigated with theoretical models based on thermodynamic considerations. Gonzalez-Bagnoli et al.[26] compared results for the thermal diffusion factor, $\alpha = TS_T$, obtained from seven thermodynamic models for the Soret effect with experimental data for three mixtures. They found that three of the older models did not provide good results for any of the mixtures and that the remaining four models had varying success in predicting the sign and magnitude of the thermal diffusion factors. Part of the problem is the quality of the equation of state. A comparison of results from different equations of state showed, in agreement with earlier work,[29] that the partial molar quantities have a large effect on the calculated values of the thermodiffusion factors. However, it was also found that an improvement in the representation of the partial molar quantities does not typically lead to improved predictions for the Soret effect.[27]

In this work, we focus on the Soret effect in binary alkane/benzene mixtures for linear as well as branched alkanes. Since benzene is a very good solvent for alkanes, we are able to explore the composition as well as temperature dependence of the Soret effect. For the *n*-alkanes, we expect the differences in the chain length (molecular mass) to have the largest effect; for the branched alkanes, we expect a significant effect due to differences in the molecular architecture and the corresponding changes in the moments of inertia. However chemical differences will also be important since the type of covalently bonded neighbors affects the interactions between carbon atoms (see, e.g., refs 29,30). In addition, ordering effects in the liquid may play a role. Interactions between benzene molecules are known to depend on the relative orientation of the molecules (see, e.g., refs 31−34). In the benzene solid at atmospheric pressure, the relative orientation of benzene molecules corresponds to the "T" configuration,[31,32] where the rings of the molecules are perpendicular to each other and the center of the second molecule lies
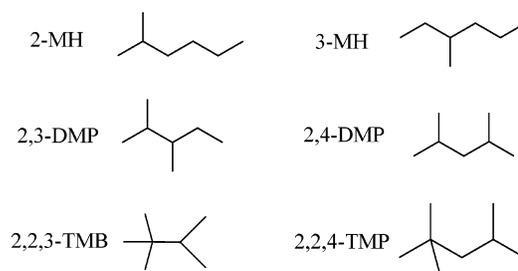

Figure 1. Chemical structure of the investigated isomers: 2-methylhexane (2-MH), 3-methylhexane (3-MH), 2,3-dimethylpentane (2,3-DMP), 2,4-dimethylpentane (2,4-DMP), 2,2,3-trimethylbutane (2,2,3-TMB), 2,2,4-trimethylpentane (2,2,4-TMP).

on the normal through the center of the ring of the first molecule.[33,34] Since the melting temperature of benzene (278.7 K) is close to the temperature of the experiments, the orientation dependence of the interactions is expected to affect the thermophysical properties of alkane/benzene mixtures.[35] The chains of normal alkanes also show some orientational order in the liquid state near the melting temperature.[36,37] While this effect is expected to be negligible for most of the alkanes investigated in this work (their melting temperature is well below room temperature) it may affect thermodiffusion for the long-chain alkanes. Since interactions between molecules play such an important role in thermal diffusion, a systematic investigation of the alkane/benzene mixtures will aid the development of molecular models for computer simulations, which have recently become an important tool in the investigation of the Soret effect (see, for example, refs 15, 38−40).

In this work, the thermal diffusion behavior of alkane/benzene mixtures is investigated experimentally with thermal diffusion forced Rayleigh scattering (TDFRS). Experiments were performed on mixtures of benzene with the linear alkanes heptane, nonane, undecane, tridecane, pentadecane, and heptadecane and with five isomers of heptane, namely 2-methylhexane, 3-methylhexane, 2,3-dimethylpentane, 2,4-dimethylpentane, and 2,2,3-trimethylbutane, and one isomer of octane, 2,2,4-trimethylpentane. The chemical structures of the investigated isomers are presented in Figure 1. Experiments were performed in a temperature range from 20 to 40 °C and for blends with alkane mole fractions of $x = 0.25$, 0.5, 0.75, and 0.85 and for a mass fraction of $x = 0.05$. The experiments yield values for the Soret coefficients, S_T, the mass diffusion coefficients, D, and the thermal diffusion coefficients $D_T = S_T D$.

In order to investigate with theoretical methods the effect of intermolecular interactions on thermal diffusion, we have adapted a recently developed two-chamber lattice model for thermodiffusion[41,42] to alkane/benzene mixtures. In the two-chamber lattice model, one considers a lattice system divided into two chambers of equal size that are maintained at slightly different temperatures. Particles are free to move between the chambers, which do not otherwise interact. The partition functions for the chambers are calculated in exact enumeration and combined to yield a sum of states for the system. The Soret coefficient is then determined from the difference in average composition of the solutions in the two chambers. The system-dependent parameters of the model are determined from a comparison with thermodynamic properties of the pure components and volume changes on mixing. This allows us to make predictions of the Soret coefficient as a function of temperature, pressure, and composition without adjustable parameters. We find that predictions from this model, which includes the effects of chain length of the alkanes and orientation-dependent

Thermal Diffusion Behavior of Alkane/Benzene Mixtures

J. Phys. Chem. B, Vol. 110, No. 51, 2006 **26217**

interactions of benzene molecules, are in good qualitative agreement with the Soret coefficients of linear alkane chains in benzene.

The paper is organized as follows: in Section II, we briefly describe the sample preparation, as well as the TDFRS experiment and the index of refraction measurements necessary for the evaluation of the TDFRS signal. In Section III, we present our experimental results for mixtures of benzene with linear and branched alkanes. In Section IV, we describe the two-chamber lattice model that is used to predict values of the Soret coefficients of *n*-alkane/benzene mixtures and we present a comparison with experimental data. Appendix A contains details about the determination of system-dependent parameters for the model. We discuss our results and conclusions in Section V.

II. Experimental Section

II.1. Sample Preparation. The alkanes heptane (99.5%), nonane (99%), undecane (98%), 2-methylhexane (98%), 3-methylhexane (98%), and 2,2,3-trimethylbutane (99%) were purchased from Fluka; tridecane (99%), pentadecane (99%), heptadecane (99%), 2,3-dimethylpentane (99%), 2,4-dimethylpentane (99%), 2,2,4-trimethylpentane (99%), and benzene (99.7%) were ordered from Aldrich. Figure 1 shows the chemical structure of the investigated isomers. The alkane mole fraction for all mixtures was adjusted by weighing the components. The TDFRS experiments require a small amount of dye in the sample. In this work, all samples contained approximately 0.002 wt % of the dye Quinizarin (Aldrich). This amount ensures a sufficient optical modulation of the grating but is small enough to avoid convection and contributions of the dye to the concentration signal. Before each TDFRS experiment, approximately 2 mL of the freshly prepared solution were filtered through 0.2 μm filter (hydrophobic PTFE) into an optical quartz cell with 0.2 mm optical path length (Helma) which was carefully cleaned from dust particles before usage.

II.2. Refractive Index Increment Measurements. In order to determine the changes of the refractive index *n* with blend composition *w* at constant pressure *P* and temperature *T*, $(\delta n/\delta w)_{P,T}$, for each alkane/benzene system measurements were performed with an Abbe refractometer for several mixture compositions around the desired molar fraction. The slope $(\delta n/\delta w)_{P,T}$ was then determined by linear interpolation. For instance, we measured the refractive index for seven concentration in the range between 0.35 and 0.75 in order to determine the slope $(\delta n/\delta w)_{P,T}$ for *x* = 0.5. An analog procedure was used for intermediate molar fractions of *x* = 0.25 and *x* = 0.75. For measurements at very low alkane concentrations, it is important to perform the index of refraction measurements using benzene from the same lot as is used in the TDFRS experiments. The reason is that the index of refraction of benzene is very sensitive to impurities. Even for high grade benzene we observed a range of refractive index values for pure benzene (between 1.500 and 1.502 at room temperature) which may lead to significant changes in the measured refractive index increment for mixtures with low alkane content. For all mixture compositions investigated in this work, the temperature derivatives at constant pressure and composition, $(\delta n/\delta T)_{P,w}$, were determined from measurements with a Michelson interferometer[43] in a temperature range of 3 °C above and below the temperature of the TDFRS experiment.

II.3. TDFRS Experiment and Data Analysis. In our thermal diffusion forced Raleigh scattering (TDFRS) experiments, the beam of an an argon-ion laser (λ_w = 488 nm) is split into two
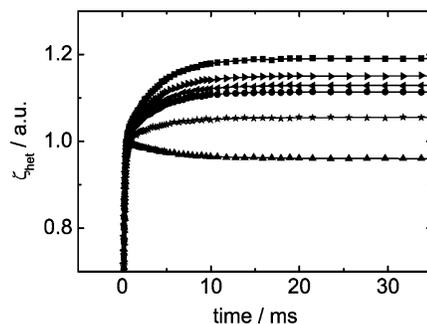
Figure 2. Typical normalized TDFRS signals for binary equimolar mixtures of heptane(square), 2-MH (right-pointing triangle), 3-MH (left-pointing triangle), 2,4-DMP (circle), 2,3-DMP (stars), and 2,2,3-TMB (upwards-pointing triangle) in benzene at a temperature of 30 °C. The solid lines represent the fits to eq 3.

writing beams of equal intensity which are allowed to interfere in the sample cell (see ref 15 for a detailed description of the method). A small amount of dye is present in the sample and converts the intensity grating into a temperature grating, which in turn, causes a concentration grating by the effect of thermal diffusion. Both gratings contribute to a combined refractive index grating, which is read out by Bragg diffraction of a third laser beam (λ_r = 633 nm).

Figure 2 shows typical heterodyne signals of the read-out laser normalized to the thermal signal. The intensity ζ_{het} (*t*) of the signal depends on the transport coefficients and the index of refraction increments and may be expressed as

$$\zeta_{\text{het}}(t) = 1 + \frac{(\partial n/\partial w)_{P,T}}{(\partial n/\partial T)_{P,w}} S_{\text{T}} w (1 - w)(1 - e^{-q^2 Dt}) \quad (3)$$

where $q = (4\pi n/\lambda_w) sin(\theta/2)$ is the grating vector, whose absolute value is determined by the angle θ between the two writing beams, the wavelength λ_w, and the index of refraction *n*.

For the determination of the transport coefficients, eq 3 is fitted to the measured heterodyne signal (see Figure 2) using the independently measured contrast factors $(\partial n/\partial w)_{p,T}$ and $(\partial n/\partial T)_{p,w}$.

III. Results

In Figure 3 we present results for the Soret coefficients S_T, the mutual diffusion coefficients *D*, and the thermal diffusion coefficients, D_T, as a function of temperature for equimolar mixtures of benzene and the six *n*-alkanes considered in this work. For the heptadecane/benzene mixture, only the Soret coefficients are shown in Figure 3 since the small amplitude of the signal at the lowest temperatures prevented a reliable determination of the mutual and thermal diffusion coefficients for this mixture. The Soret coefficients of the alkanes in Figure 3 are negative which implies that the alkane molecules tend to move to the warmer regions of the fluid while the benzene molecules tend to move in the opposite direction. With increasing chain length, the Soret coefficients increase (their magnitude decreases) and the slope of the temperature dependence decreases becoming negative at the highest molecular weights. The diffusion coefficients *D* increase with increasing temperature and decrease with increasing molecular weight of the alkane. The chain length dependence of the diffusion coefficients is expected since the size of the alkane molecules and the viscosity of the mixture increase with increasing molecular mass of the alkanes.
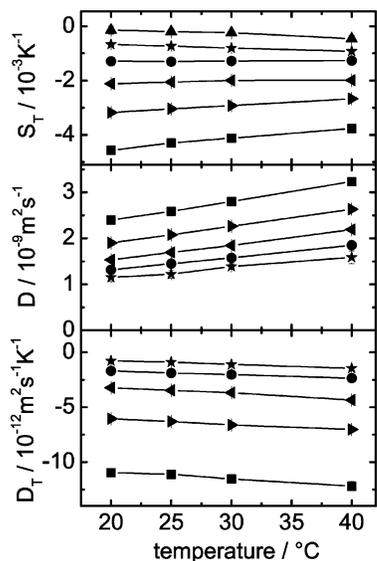
26218 *J. Phys. Chem. B, Vol. 110, No. 51, 2006*

Polyakov et al.

Figure 3. Transport coefficients for equimolar mixtures of benzene and linear alkanes as a function of temperature. The symbols indicate the Soret coefficients S_T, diffusion coefficients D and thermal diffusion coefficients D_T of heptane (square), nonane (right-pointing triangle), undecane (left-pointing triangle), tridecane (circle), and pentadecane (star) and the Soret coefficients of heptadecane (upwards-pointing triangle) in benzene. The lines connect the data points.
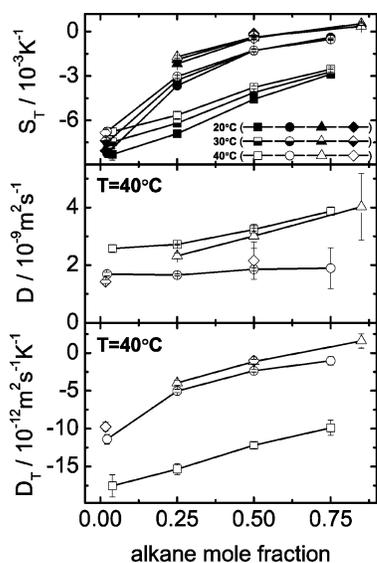

Figure 4. Soret coefficient S_T, diffusion coefficient D, and thermal diffusion coefficient D_T of heptane (squares), tridecane (circles), heptadecane (diamonds), and 2,2,4-TMP (triangles) in benzene as a function of the alkane concentration. The top panel shows results for S_T at three different temperatures as indicated. The lower panels show results for D and D_T at a temperature of 40 °C. The lines connect the data points.

Figure 4 shows the transport coefficients S_T, D, and D_T as a function of alkane mole fraction for mixtures of benzene with heptane, tridecane, and the branched octane isomer 2,2,4-trimethylpentane (2,2,4-TMP). Experimental values for three different temperatures are shown for the Soret coefficients while experimental data for a single temperature are shown for the mutual and the thermal diffusion coefficients. For each of the mixture systems, the Soret coefficient increases with increasing alkane concentration. For heptane and tridecane, the Soret coefficients remain negative for all concentrations investigated here. For 2,2,4-TMP, however, the Soret coefficient changes sign near the alkane mole fraction of $x = 0.75$ and is positive
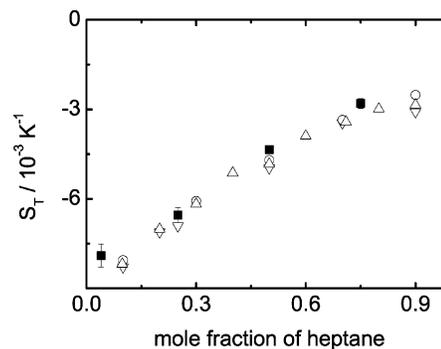

Figure 5. Soret coefficients of heptane/benzene mixtures at a temperature of 25 °C as a function of heptane mole fraction. The symbols represent experimental data by (Bou-Ali et al. [21] ($\bigtriangledown$), Korsching[17] ($\bigcirc$), Demichowicz-Pigoniowa et al. [19] ($\triangle$) and from this work ($\blacksquare$).)
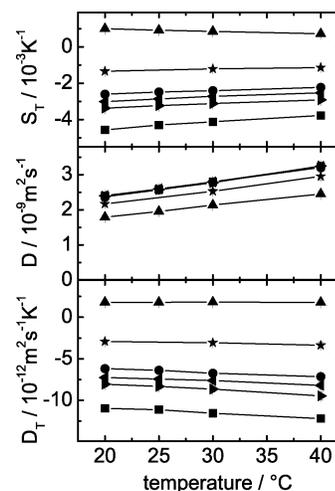

Figure 6. Soret coefficient S_T, diffusion coefficient D and thermal diffusion coefficient D_T of heptane (square), 2-MH (right-pointing triange, 3-MH (left-pointing triange), 2,4-DMP (circle), 2,3-DMP (star), and 2,2,3-TMB (upwards-pointing triangle) in benzene at a mole fraction of 0.5 as a function of the temperature. The lines connect the data points.

for $x = 0.85$. The mutual diffusion coefficient D increases with increasing alkane concentration.

Soret coefficients of heptane/benzene mixtures have been measured independently by Korsching,[17,18] Demichowicz-Pigoniowa et al.,[19] Ecenarro et al.[13] and Trevoy et al.[20] The results for a temperature of 25 °C are presented in Figure 5 as a function of heptane concentration. The figure shows satisfactory agreement between the results obtained in this work and those from the literature for a temperature of 25 °C. We also considered other temperatures and found excellent agreement with data by Korsching[18] for 35 °C and with Ecenarro et al.[13] for 37.5 °C. At the same time our data for 35 °C are 6% smaller than those of Bou-Ali et al.[21] Soret coefficients for an equimolar heptane/benzene mixture at different temperatures measured in this work agree fairly well with the data reported by Trevoy et al.[20]

Figure 6 shows the transport coefficients S_T, D, and D_T for equimolar mixtures of benzene and isomers of heptane as a function of temperature. As in the case of the linear alkanes, the Soret coefficients are negative, except for the strongly branched 2,2,3-trimethylbutane (2,2,3-TMB), which has a positive Soret coefficient. At all temperatures, we find that the Soret coefficients increase with increasing number of side groups of the isomers. This implies that branching decreases the tendency for the alkanes to move to the warmer regions of a fluid. The diffusion coefficients of heptane and the isomers

Thermal Diffusion Behavior of Alkane/Benzene Mixtures

J. Phys. Chem. B, Vol. 110, No. 51, 2006 **26219**

2-MH, 3-MH, and 2,4-DMP are the same within experimental uncertainty, while the diffusion coefficients are lower for the remaining isomers, 2,3-DMP and 2,2,3-TMB. Higher values of the viscosity may be responsible for the smaller values for the diffusion coefficient of 2,3-DMP and 2,2,3-TMB.[44]

IV. Lattice Model For The Soret Effect In Alkane/benzene Mixtures

In this work, we describe mixtures of benzene and normal alkanes with a simple lattice model that includes the effects of compressibility and orientation dependent interactions between benzene molecules. Consider a simple cubic lattice (coordination number $z = 6$) with N_L sites of which N_b and N_a are occupied by benzene and the alkane, respectively. In order to account for compressibility, some of the sites will be unoccupied so that $N_L = N_b + N_a + N_v$, where N_v is the number of voids. The total volume of the lattice is $V = vN_L$, where v is the volume of one elementary cube. Interactions between occupied nearest neighbor sites are described by interaction energies ϵ_{ij}, where the subscripts indicate the occupants of the sites (b for benzene and a for the alkane; voids are assumed to have zero interaction energies).

To account for the orientation dependence of interactions between benzene molecules in an approximate way, we introduce an orientational degree of freedom for the benzene sites on the lattice. A disk on a simple cubic lattice may be oriented so that its normal is aligned with the *x, y,* or *z*-axis. Accordingly, we assign one of three possible orientations to each site occupied by benzene. In order to distinguish between different relative orientations, we introduce two interaction energies for benzene–benzene interactions. The energy parameter $\epsilon_{bb;p}$ corresponds to preferred relative orientations of benzene molecules and is lower than the parameter $\epsilon_{bb,n}$ for the remaining orientations. A fraction f of the possible relative orientations is assumed to have the lower interaction energy. To estimate this fraction for our lattice model, consider a disk located at the origin (coordinates (0, 0, 0)) and aligned with the *z*-axis. If the nearest neighbor site (0, 0, 1) or (0, 0, −1) is occupied by another disk, then two of the three possible orientations of this disk correspond to "T" configurations with interaction energy $\epsilon_{bb;p}$. For the nearest neighbor sites (± 1, 0, 0) and (0, ± 1, 0), on the other hand, only one of three orientations of the occupying disk yields a "T" configuration. Hence, eight of the total of eighteen relative orientations corresponds to favorable interactions, which yields $f = 4/9$ for the fraction of preferred orientations.

A first approximation to the probability p_p that two benzene sites make a preferred contact at a given temperature T is given by

$$p_p = \frac{fe^{-\beta\epsilon_{bb;p}}}{fe^{-\beta\epsilon_{bb;p}} + (1 - f)e^{-\beta\epsilon_{bb;n}}} \quad (4)$$

where $\beta = 1/k_BT$ and k_B is Boltzmann's constant. With a random mixing approximation[45] for the arrangement of the different sites on the lattice, we obtain for the internal energy per site, u,

$$u = \frac{z}{2}(\phi_b^2[p_p\epsilon_{bb;p} + (1 - p_p)\epsilon_{bb;n}] + \phi_a^2\epsilon_{aa} + 2\phi_a\phi_b\epsilon_{ab}) \quad (5)$$

where the energy parameters ϵ_{aa} and ϵ_{ab} describe alkane–alkane and alkane–benzene interactions, respectively, and where ϕ_a, ϕ_b, and ϕ_v denote the fractions of lattice sites occupied by the alkane, benzene, and voids, respectively. With these approxima-

tions, the canonical partition function of the system may be written as

$$Z(N_L, T, N_a, N_b) = 3^{N_b}\binom{N_L}{N_a}\binom{N_L - N_a}{N_b}$$

$$\times \exp\left\{-\beta N_L\frac{z}{2}(\phi_b^2\tilde{\epsilon}_{bb} + \phi_a^2\epsilon_{aa} + 2\phi_a\phi_b\epsilon_{ab})\right\} \quad (6)$$

where an effective interaction parameter $\tilde{\epsilon}_{bb}$ has been introduced,

$$e^{-\beta\tilde{\epsilon}_{bb}} = fe^{-\beta\epsilon_{bb;p}} + (1 - f)e^{-\beta\epsilon_{bb;n}} \quad (7)$$

From the partition function, the pressure of the system may be calculated according to

$$P = \frac{1}{\beta v}\left(\frac{\partial Z}{\partial N_L}\right)_{N_a, N_b} \quad (8)$$

In Appendix A, we describe how the system-dependent parameters for the alkane/benzene mixtures were determined. In the following, we use a lattice with $N_L = 5000$ sites. For a given temperature, pressure, and composition of a mixture, the occupation numbers N_a and N_b are determined by gradually filling the lattice with alkane and benzene sites in the right proportion until the pressure reaches the desired value. Due to the discrete nature of the lattice, the targeted pressure cannot be reached exactly. However, the size of the lattice ensures that the deviations from the target pressure have a negligible effect on the results presented here.

IV.1. Calculation of Soret Coefficients. In order to describe thermodiffusion, we divide the lattice into two equal chambers, A and B, each with lattice sites $N^A = N^B = N_L/2$ but with slightly different temperatures, $T^A = T^B + \delta T$. With N_a and N_b denoting the alkane and benzene occupation numbers of the whole lattice, chambers A and B have occupation numbers { N_a^A, N_b^A} and {$N_a^B = N_a - N_a^A, N_b^B = N_b - N_b^A$}, respectively. Under the assumption that the chambers are non-interacting, the partition function of the whole system is the product of the partition functions of the chambers, Z^AZ^B. A sum of states Q may then be defined by summing overall possible occupations of the two lattices[41]

$$Q = \sum_{[N_a^A, N_b^A]} Z^A(N^A, T^A, N_a^A, N_b^A)$$

$$\times Z^B(N^B, T^B, N_a - N_a^A, N_b - N_b^A) \quad (9)$$

where the square brackets indicate a summation consistent with the total number of particles and lattice sites.

We evaluate eq 9 by exact enumeration of all possible occupations of the chambers. As we are performing the calculation of the terms in the sum of states, we also calculate the mass fractions of the alkane, $w^A(N_a^A, N_b^A)$ and $w^B(N_a - N_a^A, N_b - N_b^A)$ using eq A3 applied to the filling fraction of the chambers. The average mass fraction $\bar{w}^A$ of the alkane in chamber A is determined by the weighted sum

$$\bar{w}^A = \frac{1}{Q}\sum_{[N_a^A, N_b^A]} w^A(N_a^A, N_b^A)Z^A(N^A, T, N_a^A, N_b^A)$$

$$\times Z^B(N^B, T, N_a - N_a^A, N_b - N_b^A) \quad (10)$$

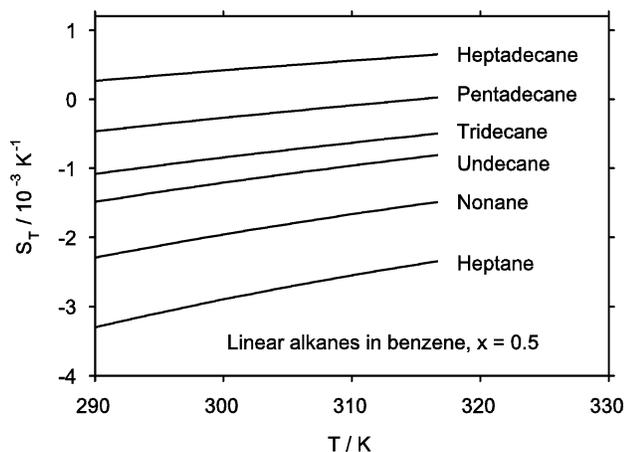and similarly for the average mass fraction $\bar{w}^B$ in chamber B.

Figure 7. Alkane Soret coefficients as a function of temperature for mixtures of benzene and linear alkanes at a mol fraction of $x = 0.5$ and atmospheric pressure. The solid lines indicate values for the Soret coefficient S_T calculated from eq 11 as described in the text.

Finally, the Soret coefficient of the alkane is calculated from

$$S_T = - \frac{1}{w(1-w)} \frac{\bar{w}^A - \bar{w}^B}{T^A - T^B} \qquad (11)$$

where w is the alkane mass fraction of the whole system.

IV.2. Comparison with Experimental Data. In Figure 7 we present predictions from our lattice model for the Soret coefficients of equimolar *n*-alkane/benzene mixtures as a function of temperature. In agreement with the experimental data shown in Figure 3, the S_T values calculated from eq 11 increase with increasing chain length. As in the case of the experimental data, the slope of the Soret coefficients as a function of temperature decreases with increasing chain length. However, at this composition, the predicted slope of S_T versus T is positive for all chain lengths, whereas the experiments show a negative slope for the longest chains. The sign of the slope is composition dependent. For low alkane concentrations, both theory and experiment show positive slopes for all chain lengths. As the alkane content increases, the slope decreases and becomes negative for the longest chains at high alkane concentration. For tridecane, for example, the experimental data presented in Figure 4 show the Soret coefficient to increase with temperature for $x = 0.25$, to be almost independent of temperature for $x = 0.5$, and to decrease with temperature for $x = 0.75$. The calculated S_T values for tridecane change from increasing with temperature to decreasing with temperature at a higher alkane content ($x \simeq 0.92$) and only after the calculated Soret coefficients have become positive. For heptadecane, the change in behavior in the experimental data occurs for a concentration smaller than $x = 0.5$ while the calculated values change behavior near $x \simeq 0.78$. Figure 8 shows Soret coefficients as a function of chain length N of the alkanes at a fixed temperature of 30 °C for the same mixtures as in Figure 7. A comparison between theory (open symbols) and experiment (filled symbols) shows that the model describes well the trend in the chain length dependence but that the calculated S_T values are always between 0.5 and 1.3×10^{-3} K^{-1} higher than the experimental values at this composition.

In Figure 9, we present Soret coefficients of heptane and tridecane in mixtures with benzene as a function of composition for three different temperatures. The symbols connected by dashed lines represent experimental data (see also Figure 4) while the solid lines represent Soret coefficients calculated from
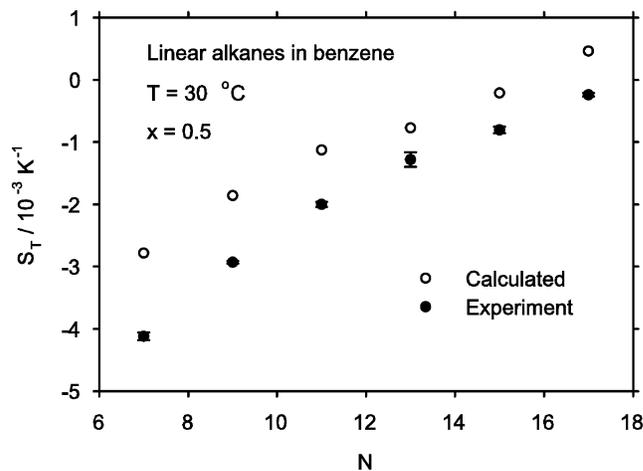

Figure 8. Alkane Soret coefficients as a function of number of carbon atoms in the alkane chain for mixtures of benzene and linear alkanes at a mol fraction of $x = 0.5$ and a temperature of 30 °C. The open symbols represent values for the Soret coefficient calculated from eq 11, the filled symbols represent experimental results from this work.
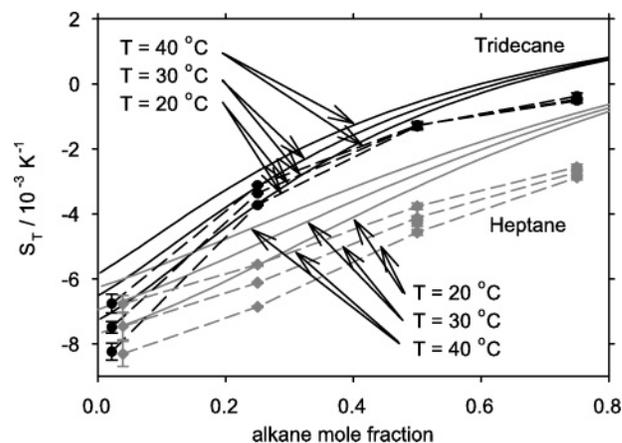

Figure 9. Soret coefficients of heptane and tridecane in mixtures with benzene as a function of composition for three different temperatures. The solid lines indicate values for the Soret coefficient calculated from eq 11, the symbols represent experimental results from this work (see Figure 4), the dashed lines connect data points.

eq 11. Both theory and experiment show an increase of the alkane Soret coefficients with increasing alkane mole fraction, x. They also show that the temperature dependence of the Soret effect is larger for benzene-rich mixtures than for alkane rich mixtures, as discussed above. As in the comparison at fixed mixture composition, the theory reproduces the trends in the experimental data but it overestimates the values of the Soret coefficients.

Experimental data are most easily interpreted for mixtures where the alkane concentration is very low. For dilute alkane mixtures, the density of the mixture is close to that of pure benzene. In addition, each alkane molecule is surrounded by benzene molecules so that interactions between alkane molecules do not play a role. For dilute solutions, our lattice model shows a close correlation between (net) interaction parameters and the Soret coefficient: the minority component is enriched in the warmer regions of the fluid (and its Soret coefficient is negative) when the contribution to the internal energy of the mixed interaction is less negative (less attractive) than that of the interactions between molecules of the majority component. The absolute value of the Soret coefficient decreases as the magnitude of the difference between contributions from mixed
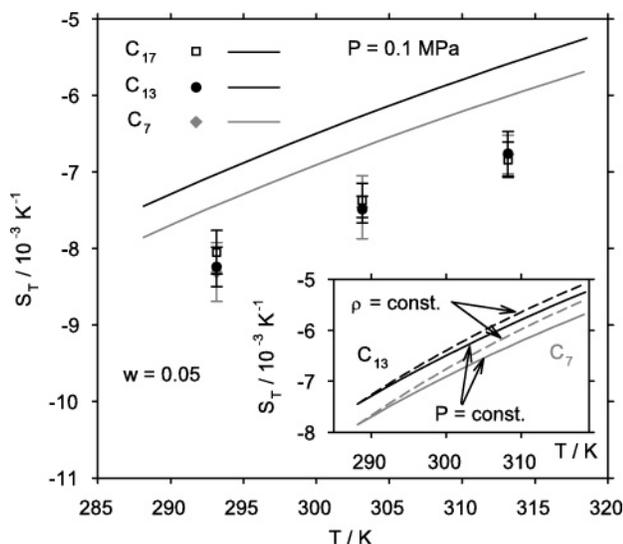
Thermal Diffusion Behavior of Alkane/Benzene Mixtures

J. Phys. Chem. B, Vol. 110, No. 51, 2006 **26221**

Figure 10. Alkane Soret coefficients as a function of temperature for mixtures of benzene and linear alkanes at a mass fraction of $w = 0.05$ and atmospheric pressure. The symbols represent experimental data for heptadecane (C_{17}), tridecane (C_{13}), and heptane (C_7). The solid lines represent values for the Soret coefficient S_T calculated from eq 11 for a pressure of 0.1 MPa for heptane (gray), tridecane (black) and heptadecane (indistinguishable from tridecane in the graph). The inset compares calculations at constant pressure, $P = 0.1$ MPa, (solid lines) with calculations at constant density (dashed lines), $\rho = 869.2$ kg/m^3 for heptane and $\rho = 874.0$ kg/m^3 for tridecane.

and like interactions decreases. For mixtures dilute in alkane, the relevant interaction energy for like interactions is the average energy associated with a benzene−benzene contact

$$\langle \epsilon_{bb} \rangle = p_p \epsilon_{bb;p} + (1 - p_p) \epsilon_{bb;n} \quad (12)$$

where the probability p_p is given by eq 4.

Figure 10 shows temperature-dependent Soret coefficients for mixtures with very low alkane mass fractions ($w = 0.05$). The symbols represent experimental data (see Figure 4) for heptadecane, tridecane, and heptane. The solid lines show calculated values for heptane, tridecane, and heptadecane, where the curves for tridecane and heptadecane are indistinguishable in this graph. The experiments on $w = 0.05$ mixtures yield negative Soret coefficients for the alkanes (heptane, tridecane, and heptadecane) with values that are independent of chain length within the uncertainty of the experiment. The observed chain-length independence may be due to a competition between two effects. For dilute solutions of chain molecules, one often observes thermal diffusion coefficients that are chain-length independent[4,6,46] and, since mutual diffusion coefficients decrease with increasing chain length, Soret coefficients whose absolute values increase with molecular mass. For the *n*-alkane/benzene mixtures at higher concentrations, on the other hand, we observe absolute values of the Soret coefficients that decrease with chain length. Additional measurements at lower and intermediate concentrations would be required to test if this competition between effects indeed takes place. The predicted values of the Soret coefficients in Figure 10 are negative and systematically higher than the experimental values. The calculated S_T values, however, show a chain length dependence for shorter chains and become independent of N when the mixed benzene−alkane interactions become chain-length independent, that is for $N = 11$ to $N = 17$ (see Table 1). In the present lattice model, there is no chain connectivity and no distinction between alkane sites at chain ends (methyl groups) and along the chain (ethyl groups). The

TABLE 1: System-Dependent Parameters for Alkane/benzene Mixtures[a]

lattice site volume $v = 2.2348 \times 10^{-5}$ m^3·mol^{-1}				
benzene	$M_{w,b}$ g·mol^{-1}	r_b	$\epsilon_{bb};p$ J·mol^{-1}	$\epsilon_{bb};n$ J·mol^{-1}
$f = 0.444$	78.11	3.7870	−4142.4	−226.87

alkane	$M_{w,a}$ g·mol^{-1}	r_a	ϵ_{aa} J·mol^{-1}	ϵ_{ab} J·mol^{-1}
heptane	100.21	6.1064	−2526.9	−2506
nonane	128.26	7.5131	−2596.4	−2526
undecane	156.31	8.9359	−2648.7	−2539
tridecane	184.37	10.311	−2659.4	−2540
pentadecane	212.42	11.755	−2696.8	−2543
heptadecane	240.48	13.225	−2743.0	−2540

[a] $M_{w,a}$ and $M_{w,b}$ denote the molecular masses, r_a and r_b the number of lattice sites per alkane and benzene molecule, respectively, ϵ_{ij} are the interaction parameters as discussed in the text, and f is the fraction of favorable benzene−benzene contacts.

differences between theoretical and experimental values suggest that such a distinction is important.

Figure 10 shows that our model reproduces the temperature dependence of the Soret coefficients for mixtures with low alkane content very well. In order to investigate the role of thermal expansion, we also performed constant density calculations for these mixtures. The inset shows as dashed lines calculated S_T values as a function of temperature for a constant density corresponding to the density at atmospheric pressure for the lowest temperature displayed. A comparison of the results from the constant pressure (solid lines) and constant density (dashed lines) calculations shows that thermal expansion of the mixtures with low alkane content leads to more negative values of the Soret coefficients for the alkanes. At constant density, the calculated temperature dependence of the Soret coefficients is a consequence of the temperature dependence of the average energy per benzene−benzene contact, eq 12. The temperature dependence at constant pressure also includes a contribution due to the density decrease with increasing temperature. For mixtures that are rich in benzene, a decrease in density leads to the disruption of mixed benzene−alkane contacts and has a similar effect as a decrease in the magnitude of the mixed interaction energy, i.e., an increase in the tendency of the alkane to move to the warmer regions of the fluid.

The concentration-dependent Soret coefficients displayed in Figures 4 and 9 show that the tendency of alkane molecules to migrate to the warmer regions of the fluid decreases (the Soret coefficients become more positive) with increasing alkane concentration for all temperatures and alkane molecules investigated. When the concentrations of alkane and benzene molecules are nearly equal, close to a weight fraction of $w = 0.5$, the differences in the interactions between like molecules dominate the Soret effect. Since benzene−benzene interactions are more attractive than alkane−alkane interactions, we observe negative Soret coefficients for all alkanes. (Please note that the values in Figure 7 are calculated for a mole fraction of $x = 0.5$ which corresponds to a mass fraction of about $w = 0.75$ for heptadecane). Part of the concentration dependence of the Soret coefficients is due to the difference in interaction energies for benzene−alkane and alkane−alkane contacts. The parameters in Table 1 show that the mixed interactions ϵ_{ab} are less attractive than the alkane−alkane interactions ϵ_{aa}. Since the number of alkane−alkane contacts increases with increasing alkane concentration, and since the difference between alkane−alkane and benzene−benzene interactions is smaller than that between mixed interactions and benzene−benzene interactions, the Soret coefficient is expected to become more positive with increasing

alkane content. In addition, the density decreases with increasing alkane composition and leads to a further increase of the alkane Soret coefficient. For high alkane concentrations, finally, the Soret effect is dominated by the difference in benzene−alkane and alkane−alkane interactions. While the TDFRS results suggest that the Soret coefficient of tridecane remains negative as the mixture becomes dilute in benzene, our calculations yield positive Soret coefficients for tridecane at high alkane content. This shows that the effective benzene−alkane interaction at high alkane content is more attractive than described by our simple lattice model.

In summary, the comparison of the predictions from our two-chamber lattice model with the experimental values for the Soret coefficients shows that the model captures the trends of the variation of the Soret coefficient with temperature, molecular mass, and composition. The differences between calculated and experimental values are most pronounced for alkane-rich mixtures. There are several reasons for the increase in the deviations between theory and experiment with increasing alkane content. For one, the random mixing approximation that we have employed in our lattice model is expected to be most appropriate for mixtures with low alkane concentrations since the concentration of both voids and alkane sites is low for these mixtures. As the alkane content increases at constant pressure, the total filling fraction decreases (with the density) and differences in the interaction energies are expected to lead to nonrandom distributions of nearest neighbor contacts. Furthermore, the lattice model for the alkanes is very simple and the determination of system-dependent parameters started from benzene, allowing only two adjustable parameters to describe the thermodynamics of the pure alkane fluids. A more sophisticated model for the alkanes that allows, for example, for different interaction energies for chain ends, sites along a linear chain, and branch points should lead to better description of the Soret effect for alkane rich mixtures and also allow us to investigate mixtures of branched alkane isomers. Unfortunately, the available thermodynamic data for the mixture systems investigated here are not sufficiently detailed to determine the system-dependent parameters for models with several interaction parameters for alkane−alkane and alkane−benzene interactions. However, our simple lattice model helps us separate molecular mass and density effects from effects due to differences in molecular interactions.

V. Discussion And Conclusion

The thermal diffusion forced Raleigh scattering experiments presented in this work have shown that the Soret effect in alkane/benzene mixtures depends on the molecular mass and structure of the alkane as well as the temperature and composition of the mixture. For the linear chains, a simple lattice model is able to reproduce the experimental trends. For the branched isomers, however, an interpretation of the data is more difficult. A comparison of the experimental data for branched heptane isomers in Figure 6 and with those for the linear chains between heptane and heptadecane in Figure 3 shows that the effect of branching on the Soret coefficients is larger than that of the molecular weight. This is not expected from the thermodynamic properties of the pure alkane fluids; the density at a given temperature, for example, depends much more strongly on the chain length than on the molecular architecture.

The moments of inertia have been shown to make an important contribution to the Soret effect for mixtures of cyclohexane and benzene isotopes,[10] see eq 2. In order to explore this effect we have calculated the moments of inertia about the
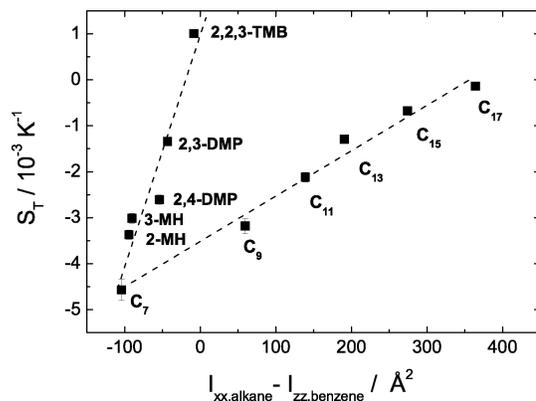

Figure 11. Soret coefficients of heptane isomers and linear alkanes as function of the difference in principle moments of inertia as discussed in the text. The symbols represent experimental values for the Soret coefficients at a temperature of 20 °C and a mole fraction of $x = 0.5$. The dashed lines are a guide to the eye.

symmetry axis (I_{zz} for the disk-like benzene molecules, I_{xx} for the more prolate alkane molecules) using an atomistic model for single molecules in vacuum.[47] In Figure 11 we present the measured Soret coefficients of the linear and branched alkanes at a temperature of 20 °C and a mole fraction of $x = 0.5$ as a function of the difference $\delta_I = I_{xx,\text{alkane}} - I_{zz,\text{benzene}}$. For the linear alkanes, there is an almost linear correlation between δ_I and the Soret coefficients. This is not unexpected since $I_{xx,\text{alkane}}$ grows almost linearly with chain length as do the Soret coefficients, which makes it difficult to separate the mass and moment of inertia contributions in eq 2. However, in contrast to what was found for the isotope mixtures, the coefficients in eq 2 representing the slope of the S_T values are not independent of composition. This suggests that a separation into mass, moment of inertia, and chemical contributions is not straightforward for the alkane mixtures.

For the branched alkanes, the moments of inertia $I_{xx,\text{alkane}}$ increase with increasing number of methyl groups much as the Soret coefficients. On the other hand, the chemical contribution is also expected to change with alkane architecture. When comparing theory and experiment for linear alkane mixtures with low alkane mass fraction ($w = 0.05$) we noted that the experimental data suggested different interaction energies between benzene molecules and methyl groups and benzene molecules and ethyl groups. Similar differences are expected to hold for interactions between different carbon groups of branched alkane molecules[29,30] and between such groups and benzene molecules. In order to investigate in more detail the origin of the large isomer effect on thermal diffusion in alkane/benzene mixtures, we are focusing in current work on dilute solutions of branched alkanes.

Appendix A: Determination Of System-Dependent Parameters For Alkane/benzene Mixtures

Our lattice model for alkane/benzene mixtures has seven system-dependent parameters. In order to determine these parameters, we consider the thermodynamic limit of the partition function introduced in eq 6 of Section IV. In this limit, eq 8 for the pressure of the mixtures yields

$$P = -\frac{1}{\beta v}\Big[\ln(1 - \phi_v) - \frac{z}{2}\beta(\phi_b^2\tilde{\epsilon}_{bb} + \phi_a^2\epsilon_a + 2\phi_a\phi_b\epsilon_{ab})\Big] \quad \text{(A1)}$$

The filling fractions are related to the density and composition of the mixture through

Thermal Diffusion Behavior of Alkane/Benzene Mixtures

J. Phys. Chem. B, Vol. 110, No. 51, 2006 **26223**

$$\phi_a = v r_a x \tilde{\rho}, \quad \phi_b = v r_b (1-x) \tilde{\rho}, \quad \phi_v = 1 - \phi_a - \phi_b \quad \text{(A2)}$$

where x is the mol fraction of the alkane and $\tilde{\rho}$ is the number density of the mixture. Here, v is the volume per lattice site and the numbers r_a and r_b represent the number of lattice sites per alkane and benzene molecule, respectively. The mass fraction w of the alkane is related to the filling fractions through

$$w = \frac{\phi_a M_{w,a}/r_a}{\phi_a M_{w,a} + \phi_b M_{w,b}/r_b} \quad \text{(A3)}$$

where $M_{w,a}$ and $M_{w,b}$ are the molecular masses of the alkane and benzene, respectively.

In eq A1, ϵ_{aa} and ϵ_{ab} are the interaction parameters for alkane−alkane and alkane−benzene interactions, respectively. The effective parameter $\tilde{\epsilon}_{bb}$ for benzene−benzene interactions was defined in eq 7 as $\exp(-\beta\tilde{\epsilon}_{bb}) = f \exp(-\beta\epsilon_{bb;p}) + (1-f) \exp(-\beta\epsilon_{bb;n})$, where $f = 4/9$ is the fraction of preferred contacts and $\epsilon_{bb;p}$ and $\epsilon_{bb;n}$ represent the interaction energies for preferred and non-preferred contacts, respectively.

For the one-component liquid benzene, we determined the system-dependent parameters v, r_b, $\epsilon_{bb;p}$, and $\epsilon_{bb;n}$ from a comparison of calculated values of thermophysical properties with tabulated values from the NIST Chemistry WebBook[48] based on the equation of state by Polt et al.[49] In the temperature range between 288 and 318 K, we considered saturated liquid densities, densities at the constant pressure of $P = 0.1$ MPa, and also at $P = 0.1$ MPa, the combination of pressure derivatives $c_p - c_v = \tilde{\rho}^{-2} T (\partial P/\partial T_{\tilde{\rho}}^2/(\partial P/\partial\tilde{\rho})_T$, where c_p and c_v are the molar isobaric and isochoric heat capacities, respectively. The resulting values for the system-dependent parameters are presented in Table 1. They correspond to a good representation of the saturated liquid densities (root mean squared relative deviation (rmsd) $\approx 0.5\%$, maximum deviation -0.78%), a very good representation of the densities at atmospheric pressure (rmsd $\approx 0.1\%$, maximum deviation 0.26%), and a reasonable representation of $c_p - c_v$ (rmsd $\approx 11\%$, maximum deviation -19%). The value of the volume per lattice site v obtained for benzene, was also adopted for the pure alkanes and for all mixtures.

For each of the alkanes, the two remaining system-dependent parameters r_a and ϵ_{aa} were determined from a comparison with tabulated values for the density at atmospheric pressure[44,50] and the corresponding thermal expansion coefficients,[44] $\alpha = \tilde{\rho}^{-1} (\partial P/\partial T)_{\tilde{\rho}}/(\partial P/\partial\tilde{\rho})_T$, in the temperature range from 288 to 318 K. The resulting values for the parameters r_a and ϵ_{aa} are included in Table 1. They correspond to a very good representation of the densities (maximum deviation -0.12%) and a reasonable representation of the thermal expansion coefficients (rmsd $\approx 9-10\%$).

Finally, in order to establish values for the mixed interaction energies ϵ_{ab}, we consider the excess molar volume V^E of alkane/benzene mixtures

$$V^E = \frac{1}{\tilde{\rho}} - \frac{x}{\tilde{\rho}_a} - \frac{1-x}{\tilde{\rho}_b} \quad \text{(A4)}$$

where $\tilde{\rho}$, $\tilde{\rho}_a$, and $\tilde{\rho}_b$ are the molar densities of the mixture, the alkane, and benzene, respectively, at the given temperature and pressure. Kouris and Panayiotou[51] measured the density of benzene, heptane, and their mixtures at a temperature of 25 °C and atmospheric pressure for a range of compositions. We determined a value for ϵ_{ab} for heptane/benzene mixtures by comparing values for the excess volume derived from the experimental data with values calculated from our lattice model. In Figure 12 we present excess volumes at 25 °C and
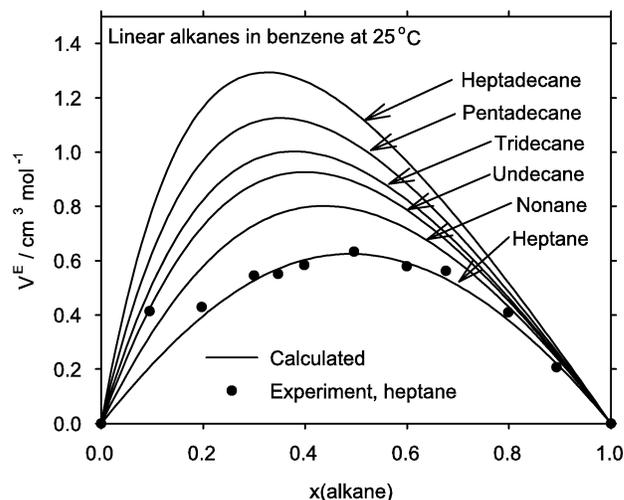

Figure 12. Excess volume of alkane/benzene mixtures at a temperature of 25 °C and atmospheric pressure. The symbols represent experimental data for heptane/benzene mixtures by Kouris and Panayiotou,[50] the lines represent values calculated from our lattice model with the parameters in Table 1.

atmospheric pressure for the mixtures of benzene with linear alkanes considered in this work. The symbols and the lowest solid line represent experimental[51] and calculated values for the excess volume of heptane/benzene mixtures, respectively, and show that the simple lattice model reproduces the volume change on mixing well. Unfortunately, excess volume data are not available for the other mixtures of benzene and *n*-alkanes considered in this work. For mixtures of benzene with the even *n*-alkanes hexane through hexadecane, Awwad et al.[52] determined excess volumes at a temperature of 25 °C and atmospheric pressure. We estimated values for the mixed interaction energies for the odd *n*-alkanes nonane through heptadecane, by requiring that the excess volumes be an increasing function of the chain length. The resulting values for the mixed interaction parameters are included in Table 1, the solid lines in Figure 12 represent values calculated with these parameters.

References and Notes

(1) Costeseque, P.; Fargue, D.; Jamet, P. In *Thermal Nonequilibrium Phenomena in Fluid Mixtures;* Köhler, W., Wiegand, S., Eds.; Springer: Berlin, 2002; Vol. LNP 584, pp 389−427.
(2) Ghorayeb K.; Firoozabadi, A. *SPE J.* **2000**, *5*, 158.
(3) Ghorayeb, K.; Firoozabadi, A.; Anraku, T. *SPE J.* **2003**, *8*, 114.
(4) Köhler, W.; Schäfer, R. In *New Developments in Polymer Analytics II, Advances in Polymer Science;* Schmidt, M., Ed.; Springer: Berlin, 2000; Vol. 151, pp 1−59.
(5) *Thermal Nonequilibrium Phenomena in Fluid mixtures, Lecture Note in Physics;* Köhler, W., Wiegand, S., Eds.; Springer: Berlin, 2002; Vol. LNP 584.
(6) Wiegand, S. *J. Phys. Condens. Matter* **2004**, *16*, R357.
(7) de Groot, S.; Mazur, P. *Non-Equilibrium Thermodynamics;* Dover: New York, 1984.
(8) Firoozabadi, A.; Ghorayeb, K.; Shukla, K. *AIChE J.* **2000**, *46*, 892.
(9) Wiegand, S.; Köhler, W. In *Thermal Nonequilibrium Phenomena in Fluid Mixtures;* Springer: Berlin, 2002; Vol. LNP 584, pp 189−210.
(10) Debuschewitz, C.; Köhler, W. *Phys. Rev. Lett.* **2001**, *87*, 055901.
(11) Wittko, G.; Köhler, W. *J. Chem. Phys.* **2005**, *123*, 014506.
(12) Zhang, K. J.; Briggs, M. E.; Gammon, R. W.; Sengers, J. V. *J. Chem. Phys.* **1996**, *104*, 6881.

(13) Ecenarro, O.; Madariaga, J. A.; Navarro, J.; Santamaria, C. M.; Carrion, J. A.; Saviron, J. M. *J. Phys.-Cond. Mater.* **1990**, *2*, 2289.

(14) Köhler W.; Müller, B. *J. Chem. Phys.* **1995**, *103*, 4367.

(15) Perronace, A.; Leppla, C.; Leroy, F.; Rousseau, B.; Wiegand, S. *J. Chem. Phys.* **2002**, *116*, 3718.

(16) Blanko, P.; Bou-Ali, M. M.; Platten, J. K.; Mandariaga, J. A.; Urteaga, P.; Santamaria, C. In *Thermodiffusion: Basics and Applications;* Bou-Ali, M., Platten, J., Eds.; 2006; p 427.

(17) Korsching, H. *Naturf. Z. a* **1974**, *29*, 1914.

(18) Korsching, H. *Z. Naturforsch A* **1969**, *24*, 444.

(19) Demichowicz-Pigoniowa, J.; Mitchell, M.; Tyrrell, H. J. V. *J. Chem. Soc. A* **1971**, p. 307.

(20) Trevoy, D. J.; Drickamer, H. G. *J. Phys. Chem.* **1949**, *17*, 1120.

(21) Bou-Ali, M. M.; Ecenarro, O.; Madariaga, J. A.; Santamaria, C. M.; Valencia, J. J. *J. Phys.-Cond. Mater.* **1998**, *10*, 3321.

(22) Leahy, A.; Firoozabadi, A. *J. Phys. Chem. B* **2006**, to be published.

(23) Platten, J. K.; Bou-Ali, M. M.; Costeseque, P.; Dutrieux, J. F.; Köhler, W.; Leppla, C.; Wiegand, S.; Wittko, G. *Philos. Mag.* **2003**, *83*, 1965.

(24) Rowley, R. L.; Yi, S. C.; Gubler, V.; Stoker, J. M. *Fluid Phase Equilib.* **1987**, *36*, 219.

(25) Rowley, R. L.; Yi, S. C.; Gubler, V.; Stoker, J. M. *J. Chem. Eng. Data* **1988**, *33*, 362.

(26) Demirel Y.; Sandler, S. I. *Int. J. Heat Mass Transfer* **2002**, *45*, 75.

(27) Gonzalez-Bagnoli, M. G.; Shapiro, A. A.; Stenby, E. H. *Philos. Mag.* **2003**, *83*, 2171.

(28) Kempers, L. J. T. M. In *Thermal Nonequilibrium Phenomena in Fluid Mixtures;* Köhler, W., Wiegand, S., Eds.; Springer: Berlin, 2002; Vol. LNP 584, pp 74−92.

(29) Rowlinson J. S.; Swinton, F. L. *Liquids and liquid Mixtures,* 3rd ed.; Butterworths: London, 1982.

(30) Chang J.; Sandler, S. I. *J. Chem. Phys.* **2004**, *121*, 7474.

(31) Schroer J. W.; Monson, P. A. *J. Chem. Phys.* **2001**, *114*, 4124.

(32) Zhao, X. S.; Chen, B.; Karaborni, S.; Siepmann, J. I. *J. Phys. Chem. B* **2005**, *109*, 5368.

(33) Walsh, T. R. *Mol. Phys.* **2002**, *100*, 2867.

(34) Cacelli, I.; Cinacchi, G.; Prampolini, G.; Tani, A. *J. Chem. Phys.* **2004**, *120*, 3648.

(35) Rubio, R. G.; Menduiña, C.; Diaz Peña, M. *J. Chem. Soc. Faraday Trans. 1* **1984**, *80*, 1425.

(36) Fischer, E. W.; Strobl, G. R.; Dettenmaier, M.; Stamm, M.; Steidle, N. *Faraday Discuss Chem. Soc.* **1979**, *68*, 26.

(37) Brambilla L.; Zerbi, G. *Macromolecules* **2005**, *38*, 3327.

(38) Rousseau, B.; Nieto-Draghi, C.; Bonet Avalos, J. *J. Europhys. Lett.* **2004**, *67*, 976.

(39) Zhang, M.; Müller-Plathe, F. *J. Chem. Phys.* **2005**, *123*, 124502.

(40) Nieto-Draghi, C.; Ávalos, J. B.; Rousseau, B. *J. Chem. Phys.* **2005**, *122*, 114503.

(41) Luettmer-Strathmann, J. *J. Chem. Phys.* **2003**, *119*, 2892.

(42) Luettmer-Strathmann, J. *Int. J. Thermophys* **2005**, *26*, 1693.

(43) Becker, A.; Köhler, W.; Müller, B. *Ber. Bunsen-Ges. Phys. Chem. Chem. Phys.* **1995**, *99*, 600.

(44) Yaws, C. L. *Chemical Properties Handbook;* McGraw-Hill: New York, 1999.

(45) Lambert, S. M.; Song, Y.; Prausnitz, J. M. Chapter 14 In *Equations of State for Fluids and Fluid Mixtures;* Sengers, J. V., Kayser, R, F., Peters, C. J., White, H. J., Jr., Eds.; Elsevier: Amsterdam, 2000; pp 523−588.

(46) Chan, J.; Popov, J. J.; Kolisnek-Kehl, S.; Leaist, D. G. *J. Solution Chem.* **2003**, *32*, 197.

(47) Chem3d, V.10, CambridgeSoft, Cambridge, MA (2006).

(48) *Nist Chemistry WebBook,* NIST Standard Reference Database 69, http://webbook.nist.gov/chemistry/ (2005).

(49) Polt, A.; Platzer, B.; Maurer, G. *Chem. Tech. (Leipzig)* **1992**, *22*, 216.

(50) Daubert, T. E.; Danner, R. P. *Physical and Thermodynamic Properties of Pure Chemicals: Data Compilation;* Hemisphere: Washington, DC, 1989−1992.

(51) Kouris, S.; Panayiotou, C. *J. Chem. Eng. Data* **1989**, *34*, 200.

(52) Awwad, A. M.; Al-Azzawi, S. F.; Salman, M. A. *Fluid Phase Equilib.* **1986**, *31*, 171.